Chapter 2
Plasmonics for Enhanced Vibrational Signatures

Katrin Kneipp, Harald Kneipp and Janina Kneipp

Abstract Vibrational signatures provide key information on the molecular composition of matter and on molecular structure and structural changes. Vibrational transitions in molecules can be probed optically by infrared absorption (IRA) and Raman scattering (RS). Exploiting local optical fields in the vicinity of plasmonic nanostructures has revolutionized optics and spectroscopy and opens up exciting new capabilities, particularly also for vibrational spectroscopy. The basic prerequisites for plasmon-supported spectroscopy are strongly enhanced and highly confined local optical fields in the wavelength range applied in the respective spectroscopic method. Here, we review plasmon supported linear and non-linear vibrational spectroscopies. Our discussion includes incoherent effects such as surface enhanced Raman scattering (SERS), surface enhanced pumped anti-Stokes Raman scattering (SEPARS), surface enhanced hyper Raman scattering (SEHRS), and surface enhanced infrared absorption (SEIRA), as well as coherent Raman techniques such as surface enhanced coherent anti-Stokes Raman scattering (SECARS) and surface enhanced stimulated Raman scattering (SESRS). Emphasis will be placed on materials and nanostructures that efficiently support various vibrational spectroscopic methods. Selected applications of surface enhanced vibrational spectroscopy for chemical probing and sensing will be discussed.

Keywords Surface plasmon · Raman scattering · SERS

K. Kneipp (✉) · H. Kneipp
Physics Department, Danmarks Tekniske Universitet, 2800 Lyngby, Denmark
e-mail: kneipp@usa.net

J. Kneipp
Chemistry Department, Humboldt Universität zu Berlin, 12489 Berlin, Germany
e-mail: janina.kneipp@chemie.hu-berlin.de

J. Kneipp
BAM Federal Institute for Materials Research and Testing, 12489 Berlin, Germany

T. V. Shahbazyan and M. I. Stockman (eds.), *Plasmonics: Theory and Applications*,
Challenges and Advances in Computational Chemistry and Physics 15,
DOI: 10.1007/978-94-007-7805-4_2,

2.1 Introduction

Building blocks of matter such as atoms in a molecule are in periodic motion and exhibit intrinsic vibrational modes. Typical vibrational frequencies range from approximately 10^{14} Hz ($\sim$3,000 cm^{-1}) for vibrations involving light atoms such as C-H groups down to the THz range ($<$100 cm^{-1}) corresponding, for example, to motions of sub-domains in proteins [1, 2]. Spectroscopic observation of vibrational modes provides a non-invasive key to the chemical composition and structure of matter. Applying vibrational spectroscopies to small quantities of matter at nanoscale dimensions and at single molecule level is a great challenge [3]. It can be met by combining vibrational spectroscopy with plasmonics and performing vibrational spectroscopy in enhanced local fields in the vicinity of plasmonic structures [4–7].

Figure 2.1 shows different processes that can be employed in vibrational spectroscopy. Molecular vibrations accompanied by changes of a dipole moment can be directly accessed by the absorption of infrared photons at the energy of the molecular vibration $h\nu_M$. Alternatively, photons can be scattered inelastically on the vibrational quantum states. As a consequence of this so-called Raman scattering process incident photons $h\nu_L$ lose energy by exciting vibrational quanta at energy $h\nu_M$, and the scattered light appears at a lower (Stokes) frequency $\nu_S = \nu_L - \nu_M$. By interacting with a molecule in an excited vibrational state, incoming photons gain energy from molecular vibrations, and the scattering signal appears at higher (anti-Stokes) frequency $\nu_{aS} = \nu_L + \nu_M$. Probing of vibrational modes by Raman scattering requires changes of polarizability α with the vibrational coordinate Q. At extremely high intensities, two photons can be simultaneously scattered by a molecular vibration. This scattering process, called hyper Raman scattering (HRS) results in an incoherent Raman signal ν_{hS} shifted relative to the twice of the excitation frequency ν_L with $\nu_{hS} = 2\nu_L - \nu_M$ or, for anti-Stokes hyper Raman scattering $\nu_{haS} = 2\nu_L + \nu_M$ [8, 9]. Following one- and two-photon excitation, respectively, the spontaneous Raman- and hyper Raman scattering processes generate an incoherent Raman signal.

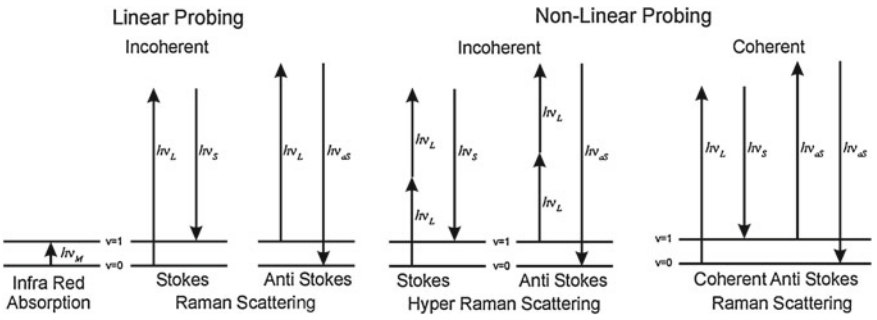

Fig. 2.1 Spectoscopic methods for probing vibrational transitions displayed in an energy level diagram, v= 0 and v= 1 are vibrational ground and first excited vibrational states

In addition to incoherent, spontaneous Raman scattering, vibrational modes can be probed by coherent Raman processes, also called stimulated, Raman scattering. There, molecular vibrations are coherently driven by two interacting fields at frequency differences that match vibrational transitions [10, 11]. In coherent Raman probing, vibrational information appears in strong and directed coherent optical signals. This makes coherent Raman scattering attractive for fast collection of vibrational information and for vibrational imaging [12]. Moreover, time resolved coherent Raman techniques, such as impulsive stimulated Raman spectroscopy or femtosecond stimulated Raman spectroscopy can provide information on the pathways and dynamics of chemical reactions, as they allow to monitor vibrational signatures of intermediate structures with ultrafast time resolution [13–16].

In this article, we focus on *surface enhanced* vibrational spectroscopy exploiting enhanced local fields of plasmonic structures. In Sect. 2.2, we introduce the incoherent effects of surface enhanced Raman scattering (SERS), surface enhanced infrared-absorption SEIRA, surface enhanced pumped anti- Stokes scattering (SEPARS), and surface enhanced hyper Raman scattering (SEHRS). There, we also explain the coherent Raman techniques of surface enhanced coherent anti-Stokes Raman scattering (SECARS) and surface enhanced stimulated Raman scattering (SESRS), and summarize some important features of these plasmonic supported optical effects. In Sect. 2.3, we discuss important properties of plasmonic nanostructures and conditions suitable for enhancing different vibrational spectra obtained in different wavelength ranges. In Sect. 2.4, we illustrate the capabilities of plasmon supported vibrational spectroscopy by selected applications, in particular ultrasensitive SEIRA of protein monolayers, monitoring of catalytic reactions on composite nanostructures with SERS, and a new class of nanosensors and labels based on SERS-, SEHRS- or SECARS signals. These examples illustrate how plasmonics transforms vibrational spectroscopy from a method for chemical structure analysis to a versatile tool providing information on chemical structures and processes along with ultrasensitive detection limits and nanoscale confinement of spectroscopic information. Section 2.5 gives a brief summary and outlook to potential future developments in the field.

2.2 “Normal” and “Surface-Enhanced” Vibrational Spectroscopy

Vibrational modes can be probed based on absorption and inelastic scattering of photons, as discussed above. Due to the Raman scattering process, vibrational information occurring in the infrared range of the spectrum is transferred to the visible, NIR, or UV range, respectively, depending on the excitation wavelength applied. Figure 2.1 illustrates some of the different spectroscopic methods for vibrational probing in an energy level diagram. Usually, in Raman scattering, excitation and/or scattered photons are not in resonance with any real molecular electronic transition (see Fig. 2.1). In contrast, in resonance Raman scattering (RRS), the excitation laser,

and often also the Raman scattered photons, match electronic transitions in the molecule. This gives rise to a stronger Raman signal for those vibrational modes which are related to the electronic transition. But, fluorescence may be excited at the same time, together with the Raman scattering, and the strong fluorescence signal can interfere with the Raman Stokes light.

A critical parameter that determines the applicability of a spectroscopic effect for structural probing is its cross section. Raman cross sections range from 10^{-31} to 10^{-29} cm^2 per molecule. In the case of RRS, cross sections become typically 2–6 orders of magnitude larger. Infrared absorption appears at cross sections from 10^{-22} up to 10^{-20} cm^2, i.e. about 10 orders of magnitude larger than non-resonant Raman cross sections. Overall, even the best cross sections achievable for vibrational spectroscopy are still orders of magnitude below those used in electronic absorption and in fluorescence which can be typically obtained at cross sections of 10^{-17}–10^{-16} cm^2. Despite the high molecular structural information content in vibrational spectra, the low cross sections, particularly those of Raman scattering, represent a considerable disadvantage for all applications of vibrational spectroscopy. This applies particularly for two-photon excitation. Cross sections on the order of 10^{-65} cm^4 s/photon for HRS—compared to 10^{-50} cm^4 s/photon typical of two-photon fluorescence—make the utilization of HRS as a practical spectroscopic tool nearly impossible. This situation has changed dramatically during the last 15 years. Exciting opportunities for gaining and improving vibrational signals arise, when spectroscopy takes place in strongly enhanced local optical fields of plasmonic nanostructures [4, 17, 18]. Field enhancement in such metal structures can be understood in terms of resonant excitation of high-Q-factor surface plasmon polaritons or/and by field concentration due to the lightening rod effect [19]. Some effects and observations exploiting enhanced optical fields, can be explained by looking at metal nanostructures as optical nanoantenna which can direct and further enhance local optical fields. [20, 21]. We discuss "surface enhancement" for different vibrational spectroscopic methods in more detail in the following sections.

2.2.1 Surface Enhanced Raman Scattering

Surface-enhanced Raman scattering (SERS) is probably the most prominent observation to demonstrate the capabilities of plasmon supported spectroscopy.

In analogy to normal, non-surface–enhanced Raman scattering, the number of Stokes photons per second n_S^{SERS} in surface-enhanced Raman scattering can be calculated as

$$n_S^{SERS} = N_0 \sigma^{SERS} n_L \tag{2.1}$$

where σ_S^{SERS} describes an effective cross section of the surface enhanced Raman process, S denotes the Stokes scattering. n_L is the Photon flux density of the excitation laser. N_0 is the number of molecules in the vibrational ground state, which are involved in the SERS Stokes process. The cross section for Raman scattering is

proportional to the square of the change of polarizability α with the vibrational coordinate Q. It is generally agreed that both so-called "electromagnetic" field enhancement effects and "chemical first layer" effects contribute to surface enhanced Raman signals [22]. The chemical effects include enhancement mechanism(s) of the Raman signal that can be explained in terms of specific interactions, i.e. electronic coupling between molecule and metal [23–25], resulting in a larger Raman cross section of the adsorbed molecule $\sigma^{RS}{}_{ads}$ compared to that of the molecule without coupling to the metal $\sigma^{RS}{}_{free}$. The electromagnetic field enhancement arises from the enhanced local optical field at the location of the molecule in the vicinity of a plasmonic nanostructure [18, 26, 27]. It can be described by field enhancement factors A(ν). Using these field enhancement factors for the excitation and scattered fields, an effective SERS cross section can be written as

$$\sigma^{SERS} = \sigma^{RS}_{ads} \left|A\left(\nu_L\right)\right|^2 \left|A\left(\nu_S\right)\right|^2 \tag{2.2}$$

with

$$\left|A\left(\nu\right)\right|^2 = \frac{\left|E\left(\nu\right)\right|^2}{\left|E^{(0)}\left(\nu\right)\right|^2} \tag{2.2a}$$

where E(ν) is the local optical field (laser and the scattered field, respectively), and $E^{(0)}(\nu)$ are the same fields in the absence of the metal nanostructures.

The SERS enhancement factor G_{SERS} for Stokes scattering is determined by the ratio of the effective SERS cross section σ^{SERS} to the normal Raman cross section $\sigma^{RS}{}_{free}$

$$G_{SERS} = \frac{\sigma^{RS}_{ads}}{\sigma^{RS}_{free}} \left|A\left(\nu_L\right)\right|^2 \left|A\left(\nu_S\right)\right|^2 \tag{2.3}$$

The first term in formula (2.3), $\sigma^{RS}{}_{ads}/\sigma^{RS}{}_{free}$, describes the chemical enhancement effect. Chemical SERS enhancement factors may contribute to the total SERS enhancement at a factor of 10 to 1,000. The second two terms describe the local field enhancement effect for the excitation and scattered fields, respectively. Both incoming excitation light and scattered light are enhanced, and—assuming the field enhancement being roughly the same for the excitation and scattering frequency—the electromagnetic enhancement scales roughly with the field enhancement factor to the power of four. Numerous experimental and theoretical studies show that local field enhancement constitutes the major contribution to the SERS effects by providing enhancement factors up to 10^{12}. With a contribution of an enhancement factor of $\sim 10^2$ due to a chemical SERS effect, total SERS enhancement factors can be on the order of 10^{14}. This brings typical non-resonant Raman cross sections to effective SERS cross sections on the order of 10^{16} cm^2.

2.2.2 Surface Enhanced Infrared Absorption

In principle, all photon-driven processes should benefit from enhanced local optical fields, and in fact, successful attempts to increase IR absorption signals were reported only a few years after the discovery of SERS [28]. The sensitivity of infrared (IR) vibration spectroscopy can be enhanced by several orders of magnitude if plasmonic electromagnetic nearfield enhancement is exploited. In contrast to scattering, where at least two photons are involved, SEIRA signals, as the result of a one-photon absorption process, benefit from local field enhancement $A(\nu)$ only to the power of two. The enhancement factor for infrared absorption can be written as

$$G_{SEIRA} = \frac{\sigma_{ads}^{abs}}{\sigma_{free}^{abs}} \left| A\left(\nu_M\right) \right|^2 \tag{2.4}$$

with infrared absorption cross sections $\sigma^{abs}{}_{ads}$ and $\sigma^{abs}{}_{free}$ for the free and adsorbed molecule, respectively. $A(\nu_M)$ describes the enhancement of the infrared optical field at the frequency of the vibrational transition. The cross section of IR absorption is proportional to the square of the change of the dipole moment μ with the vibrational coordinate Q. By analogy with Raman scattering, we take into account that also IR absorption cross sections may differ for adsorbed and free molecules, i.e. there may exist also a chemical contribution to SEIRA. The key prerequisites for exploiting SEIRA in practical spectroscopy are structures which provide field enhancement also in the IR range. With the concept of a novel resonant mechanism involving the interference of a broadband plasmon with the narrowband vibration from molecules, enormous enhancement of the vibrational signals from less than one attomol of molecules on individual gold nanowires was experimentally demonstrated [29, 30]. The tailored gold nanowires act as plasmonic nanoantennas in the infrared. It was demonstrated that field enhancement in the IR range can be generated by nanoparticle arrays that display shifted and broad plasmon resonances in the near to mid-IR [7, 31, 32]. Best SEIRA enhancement factors have been reported to be $10^4 - 10^5$ [7, 30]. Another approach for generating enhanced and confined local fields in the IR range exploits resonances with phonon polaritons [33, 34]. Enhancement factors of 100 for IR absorption on polar dielectric silicon carbide nanoparticles have been reported [34].

2.2.3 Surface Enhanced Raman Scattering Using Two-Photon Excitation: Surface Enhanced Hyper Raman Scattering

Hyper Raman scattering results in incoherent Raman signals shifted relative to twice the excitation frequency (see also Fig. 2.1). Hyper Raman scattering is related to higher order terms in the induced dipole moment which become operative at high

optical field strength

$$P_{ind} = \alpha E + \beta EE + \cdots \tag{2.5}$$

with β as hyper polarizability. The first linear term including α describes linear Raman and Rayleigh scattering, the second term describes *hyper* Rayleigh and *hyper* Raman scattering. Hyper Raman scattering follows symmetry selection rules different from Raman scattering. Therefore, it can probe vibrations hat are forbidden in Raman scattering [8, 9].

As a non-linear, two-photon excited process, HRS depends on the excitation photon flux density n_{L} to the power of two. In analogy to Eq. (2.1) , the number of surface-enhanced hyper Raman Stokes photons n^{SEHRS} can be calculated as

$$n^{SEHRS} = N_0 \sigma^{SEHRS} n_L^2 \tag{2.6}$$

where σ^{SEHRS} is the effective cross section of the surface-enhanced hyper Raman process.

HRS can be enhanced in an analogous fashion to normal Raman scattering by a chemical effect and by enhancement of the optical fields when the molecule is in close proximity of metallic nanostructures. The effective surface-enhanced hyper Raman cross section can be written as

$$\sigma^{SEHRS} = \sigma_{ads}^{HRS} \left|A\left(\nu_L\right)\right|^4 \left|A\left(\nu_{hS}\right)\right|^2 \tag{2.7}$$

where $\sigma^{\mathrm{HRS}}{}_{\mathrm{ads}}$ describes an "chemically" enhanced hyper Raman cross section compared to that of a "free" molecule, $\mathrm{A}(\nu)$ describe the enhancement of the optical fields at the excitation and hyper Raman scattered wavelengths, respectively. We can write an enhancement factor for SEHRS as

$$G_{SEHRS} = \frac{\sigma_{ads}^{HRS}}{\sigma_{free}^{HRS}} \left|A(\nu_L)\right|^4 \left|A(\nu_{HS})\right|^2 \tag{2.8}$$

Strong surface enhancement corresponding to the field enhancement factor to the power of six can overcome the inherently weak nature of hyper-Raman scattering and enable to measure hyper Raman spectra also at the anti-Stokes side [35].

Figure 2.2 displays Stokes and anti-Stokes hyper Raman spectra and illustrates the dependence of non-linear SEHRS signals on the excitation intensity to the power of two. Effective cross sections of SEHRS have shown to be on the order of $10^{-46} - 10^{-45}\,\mathrm{cm}^4\,\mathrm{s}$, comparable or even better than the best cross sections for two-photon fluorescence obtained so far. These cross sections enable the measurement of SEHRS spectra at excitation intensities of $10^6 - 10^7\,\mathrm{W}\,/\,\mathrm{cm}^{-2}$, conditions that can be easily achieved with mode-locked picosecond lasers under weak focusing conditions [36], and also in tightly focused continuous wave (cw) [37] or low-energy pulsed lasers [38].

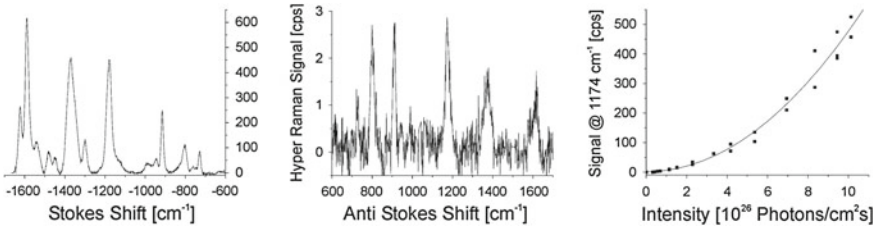

Fig. 2.2 **a** SEHRS Stokes and anti-Stokes spectra of crystal violet attached to silver nanoaggregates. The spectra were measured using 1,064 nm mode locked ps pulses at an average power of 40 mW. Anti-Stokes HRS can be observed because of the extremely high effective cross section of SEHRS. **b** The square-law dependence of the hyper Raman scattering signal on the excitation intensity verifies the two-photon process. *cps* counts per second (Reprinted with permission from [35])

2.2.4 Surface Enhanced Pumped Anti-Stokes Raman Scattering

Anti-Stokes Raman scattering starts from the first excited vibrational levels (see Fig. 2.1) and is proportional to the number of molecules in the first excited vibrational state N_1. This number N_1, relative to the number of molecules in the vibrational ground state N_0 is determined by the Boltzmann factor. This results in much weaker anti-Stokes Raman signals than Stokes signals. A strong surface-enhanced Raman Stokes process with an effective cross section σ^{SERS} populates the first excited vibrational levels in addition to thermal population [39–42], and results in an increase of anti- Stokes signals. Under stationary conditions and in a weakly saturating intensity regime ($\exp(-h\nu_M/kT) \leq \sigma_S^{\mathrm{SERS}}\, \tau_1\, n_L << 1$), the anti-Stokes signal n_{aS}^{SERS} can be estimated according to

$$n_{aS}^{SERS} = N_0 e^{-\frac{h\nu_M}{kT}} \sigma^{SERS} n_L + N_0 \left(\sigma^{SERS}\right)^2 \tau_1 n_L^2 \tag{2.9}$$

The first term describes anti-Stokes scattering related to thermal population of the first excited vibrational state. The second term describes an anti-Stokes signal related to a population of the first excited vibrational state due to "pumping" by a spontaneous Raman Stokes process, τ_1 is the lifetime of the excited vibrational state. Pumping of vibrational levels by a surface-enhanced Stokes process in the weakly saturating intensity regime gives rise to a quadratic dependence of the anti-Stokes signal on the excitation intensity. This nonlinear pumped anti- Stokes scattering can be described by an effective two-photon cross section σ^{SEPARS}.

$$\sigma^{SEPARS} = \left(\sigma^{SERS}\right)^2 \tau_1 \tag{2.10}$$

Assuming a SERS cross section of approximately $10^{-16}\,\mathrm{cm}^2$ and a vibrational life time on the order of 10 picoseconds, effective two-photon cross sections can be up to $10^{-43}\,\mathrm{cm}^4\,\mathrm{s}$. This is about seven orders of magnitude larger than typical cross sections for two-photon excited fluorescence. Moreover, anti-Stokes spectra provide

vibrational information at the high energy side of the excitation laser, which is free from disturbing fluorescence.

SEPARS generates an incoherent anti-Stokes signal. The large effective cross section can be explained by the nature of the process, which is a two-photon process using the vibrational level as a real intermediate state. The effective Raman cross section strongly benefits from enhanced local fields. In an analogous fashion to formula (2.2), we can split chemical and electromagnetic enhancement and write the effective surface-enhanced cross section for pumped anti-Stokes scattering as

$$\sigma^{SEPARS} = \left(\sigma_{ads}^{RS}\right)^2 \tau_1 \left|A\left(\nu_L\right)\right|^4 \left|A\left(\nu_S\right)\right|^2 \left|A\left(\nu_{aS}\right)\right|^2 \tag{2.11}$$

Pumped anti-Stokes Raman scattering benefits from enhanced local fields to the power of eight. Observing the effects of vibrational pumping without support of plasmonics means dealing with an effective cross section of 10^{-71} cm^4 s. Excitation intensities on the order of 10^{20} W/cm^2 would be required in order to bring the pumped anti-Stokes signal to the level of anti-Stokes scattering from thermally (room temperature) populated vibrational modes.

2.2.5 *Surface Enhanced Coherent or Stimulated Raman Scattering Methods*

The development of lasers has triggered the field of stimulated or coherent Raman spectroscopy, also called "active Raman spectroscopy" , in the seventies of the last century [43]. Coherent Raman methods came back to the focus of interest during the recent decade [10, 11, 44].

In stimulated or coherent Raman probing, two optical fields coherently drive a vibrational mode while one of these fields, or another third one, probes this coherent molecular vibration. The third-order non-linear susceptibility $X^{(3)}$, which enables the process, has resonances at the vibrational frequencies and therefore, by tuning the frequency differences between the lasers, on can probe the vibrational spectrum of a molecule.

There are different ways to perform coherent nonlinear Raman probing. The two mostly prominent coherent Raman methods are coherent anti-Stokes Raman spectroscopy (CARS) and stimulated Raman spectroscopy (SRS): During CARS, an excitation laser (v_L) and a Stokes laser (v_S) generate a coherent molecular vibration. The excitation laser is scattered again on this vibration and produces a coherent anti-Stokes signal. The nonlinear polarization, which is responsible for CARS can be written as

$$P^{CARS} \propto X^{(3)} E_L\left(\nu_L\right) E_L\left(\nu_L\right) E_S^*\left(-\nu_S\right) \tag{2.12a}$$

In contrast, so-called stimulated Raman spectroscopy (SRS) measures changes in the signal levels of the two lasers which occur due to their non-linear interaction.

The nonlinear polarization, which generates SRS is

$$P^{SRS} \propto \mathrm{X}^{(3)} E_L\,(\nu_L)\, E_L^*\,(-\nu_L)\, E_S\,(\nu_S) \tag{2.12b}$$

Stimulated Raman spectroscopy can be used in an enhancing or depletion modus by measuring an enhancement in the lower frequency "Stokes" laser field (stimulated Raman gain), or a depletion in the higher frequency "anti-Stokes" laser field (stimulated Raman loss or inverse Raman scattering), respectively [11, 14]. Whereas CARS requires additionally phase matching conditions between the interacting lasers, stimulated Raman spectroscopy always fulfills this momentum conservation automatically.

In the discussed coherent Raman processes, four interacting coherent optical fields can benefit from plasmonic enhancement. The enhancement factor for the coherent non-linear Raman processes can be written as

$$G_{SECARS} = \frac{(\mathrm{X}^{(3)}_{ads})^2}{(\mathrm{X}^{(3)}_{free})^2}\, |A\,(\nu_L)|^4\, |A\,(\nu_S)|^2\, |A\,(\nu_{aS})|^2 \tag{2.13a}$$

$$G_{SESRS} = \frac{|\mathrm{X}^{(3)}_{ads}|^2}{|\mathrm{X}^{(3)}_{free}|^2}\, |A\,(\nu_L)|^4\, |A\,(\nu_S)|^4 \tag{2.13b}$$

Here we consider that also the non-linear susceptibility can be different for adsorbed and "free" molecules.

There are some reports on experimental demonstration of surface enhanced coherent Raman spectroscopy (SECARS) [45–50]. Silver nanoparticle aggregates, silver films and nanostructured gold surfaces were used as plasmonic enhancing structures. SECARS enhancement factors exceeding five orders of magnitude have been observed [49]. Recently, surface enhanced femtosecond stimulated Raman spectroscopy has been reported exploiting gold nanoantenna with embedded Raman molecules. Using a picosecond Raman and femtosecond probe pulse, the time- and ensemble averaged enhancement factor was estimated in the range from $10^4 - 10^6$ [51].

Figure 2.3 summarizes different plasmon supported spectroscopic methods for vibrational probing. Note that in incoherent probing, spectroscopic signals linearly depend on the number of molecules while coherent Raman signals show a quadratic dependence. In general, field enhancement factors $\mathrm{A}(\nu)$ depend on frequency. However, Raman shifts are relatively small and therefore, we can assume for SERS, SEPAS and SECARS that $\mathrm{A}(\mathrm{v_L}) \sim \mathrm{A}(\mathrm{v_S}) \sim \mathrm{A}(\mathrm{v_{aS}}) = \mathrm{A}(\nu)$. SEIRA, SERS and SEHRS depend on field enhancement factors $\mathrm{A}(\nu)$ to the power of two, four and six respectively, while SEPARS, SECARS, and SESRS benefit from $\mathrm{A}(\nu)$ to the power of eight.

For supporting different vibrational spectroscopic methods, field enhancement is required within very different wavelength ranges including IR and THz frequencies

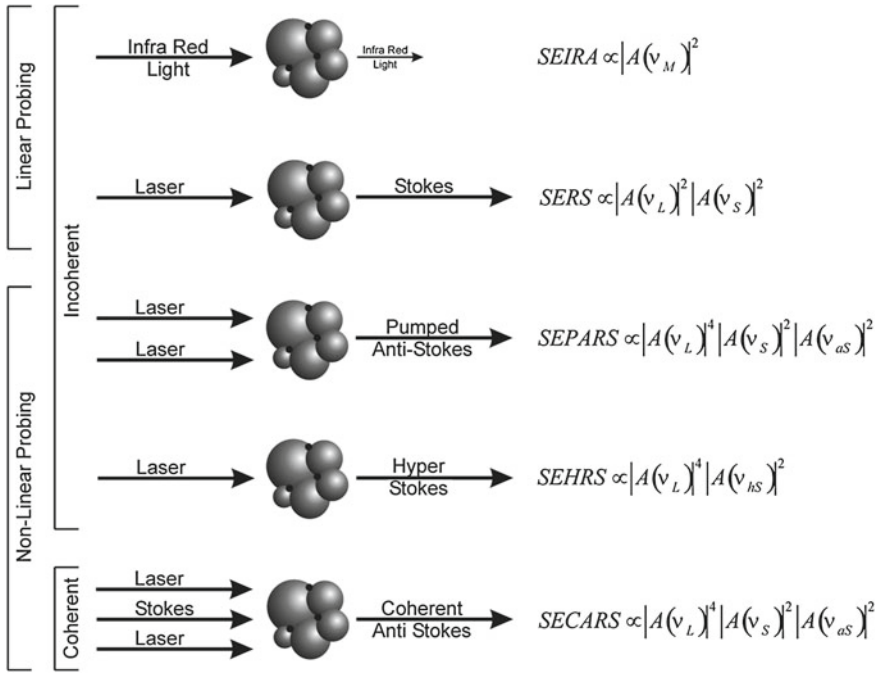

Fig. 2.3 Surface enhanced vibrational spectroscopies and their dependence on field enhancement factors A(ν)

for SEIRA and near infrared, visible or near ultraviolet frequencies for linear and non-linear (resonance) Raman scattering. For SEHRS, optimum structures should provide high enhancement in two relatively widely separated ranges of the electromagnetic spectrum. In the Sect. 2.3, we discuss basic requirements for plasmonic nanostructures suitable for surface enhanced vibrational spectroscopy.

2.3 Plasmonic Nanstructures for Supporting Vibrational Spectroscopy

The basic property of enhancing plasmonic structures is their capability to generate spatially confined and enhanced fields due to resonances with the collective oscillations of the free conduction electrons in the metal, so-called surface plasmons. This requires nanostructures with plasmon resonances in different ranges in the electromagnetic spectrum. Moreover, in order to achieve high enhancement levels, the plasmonic elements should have high Q-factors. For a modern summary about the field of nanoplasmonics, see e.g. [19, 52–55]. The existence of surface plasmons strongly depends on the dielectric constants of the metal ε_m and requires negative

real part of the complex dielectric constant, $\mathrm{Re}\,\varepsilon_m < 0$. High Q-factors, i.e. small damping requires small imaginary parts of ε_m. Gold, silver and also copper fulfil these requirements in the visible and near infrared range. Silver and gold are the most common materials in plasmon supported optics and spectroscopy. There is a strong interest in extending the working range of plasmonics by looking for new materials. For an overview of plasmonic materials see [56].

Properties of surface plasmons and related local optical fields in the vicinity of plasmonic structures are not only determined by their material properties, but also by the morphology of the structures. For example, so-called hot spots which provide extremely strong SERS enhancement always exist for aggregates formed by silver or gold nanoparticles but not for isolated particles [57, 58]. For illustration, Fig. 2.4 compares SERS experiments performed on isolated gold nanospheres and on small aggregates formed by these spheres.

In agreement with theory, enhancement factors for isolated gold spheres have been inferred to be $10^3 - 10^4$ by comparing surface enhanced Raman signals with non-surface enhanced standards. These SERS enhancement factors are too small to measurably populate the first excited vibrational state and the anti-Stokes spectrum appears at the expected relatively low signal level (Fig. 2.4b). In particular, the high frequency modes are not seen on the anti-Stokes side due to their low thermal population. This situation changes when the particles form aggregates. Now a strong anti-Stokes signals appears, in particular also for higher frequency Raman modes. This is an indication of a very strong Raman process that populates the first excited vibrational state. The difference in SERS enhancement levels for isolated

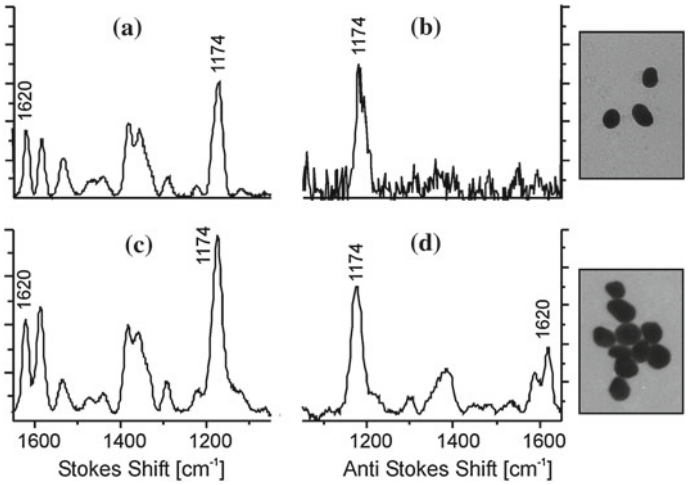

Fig. 2.4 Stokes and anti-Stokes SERS spectra of crystal violet attached to isolated and aggregated gold nanospheres. Strong anti-Stokes signals for aggregated spheres indicate population of first excited vibrational states beyond Boltzmann distribution. This population pumping due to a very strong SERS Stokes process indicates a dramatic increase in local field enhancement for nanoparticle aggregates versus isolated particles (Reprinted with permission from [58])

gold nanoparticles and aggregates can be up to 10 orders of magnitude. Isolated silver nanoparticles and silver nanoaggregates show basically the same behavior [59, 60]. The dramatic increase in field enhancement level can be explained by the interaction and hybridization of plasmons in adjacent nanoparticles [55]. Plasmonic field enhancement exhibits particularly exciting properties for fractal metallic nanostructures [61–64].

Surface plasmon resonances for isolated particles strongly depend on their shape and size. Advances in a controlled production of gold and silver nanoparticles make it possible to tune their plasmon resonances over wide ranges in the visible and NIR. Figure 2.5 summarizes representative tuning ranges for selected gold- and silver nanostructures [65].

While plasmon resonances mainly cover the range between near ultraviolet (UV) and near IR, further developing of SEIRA as a spectroscopic tool requires nanostructures which provide high field enhancement in the IR range. Nanoshells are very interesting "single-particle" plasmonic structures exhibiting well-defined tunable plasmon resonances over wide energy ranges down to the IR [66]. These structures are of particular interest for the design of enhancing structures for SEIRA experiments [31, 55, 67]. Also metal nanowires provide sufficiently strong antenna-like plasmonic resonances in the IR [29]. The resonance of the antenna can be adjusted to the molecular vibration frequencies by changing the wire length. Arrays where antennae can couple via nanogaps have been suggested and demonstrated as structures which provide strong electromagnetic enhancement in the IR range [7, 30]. Vibration-signal enhancement up to 500,000 have been obtained for molecular monolayers adsorbed on gold nanowires.

Another methodological challenge in vibrational spectroscopy is plasmonic supported (resonance) Raman scattering using ultraviolet light for excitation. The exten-

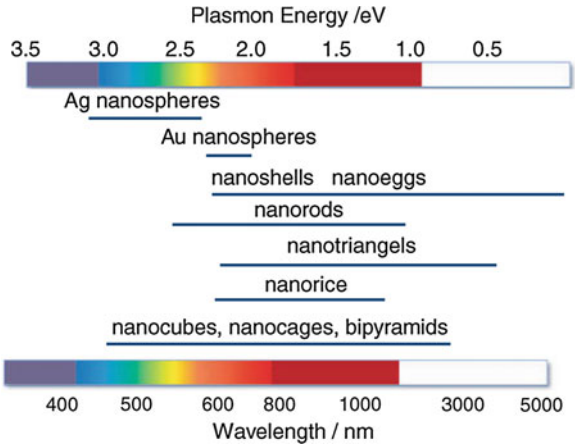

Fig. 2.5 Spectral dependence of the plasmon resonance of differently shaped silver and gold nanoparticles (Reprinted with permission from [65])

sion of SERS studies to the ultraviolet region, i.e. UV-SERS would offer interesting capabilities, particularly for supporting UV resonance Raman studies in biosciences [68, 69]. Aluminium has been considered as one of the best candidates for enhancing local fields in the UV region [70]. It has been experimentally demonstrated that Al triangular nanoparticle arrays can support plasmon resonances that are tunable throughout the visible and into the UV portion of the spectrum [71]. UV-SERS using ordered Al nanohole arrays are theoretically proposed and simulated by using FDTD method [72]. SERS spectra observed from crystal violet on aluminium using 244 nm excitation have been reported [73]. Surface-enhanced Raman scattering in the ultraviolet spectral region was also observed on rhodium and ruthenium electrodes [74].

Non-linear vibrational probing, such as hyper Raman spectroscopy can require plasmonic support in very different frequency ranges since the scattering signals appears shifted relatively to the second harmonic frequency of the excitation laser. The problem can be addressed by using enhancing structure that exhibit plasmon excitations over a wide spectral range. For example, silver aggregate structures can show a broad plasmon spectrum from 400 to 1,200 nm which covers all optical fields participating in the non-linear Raman effect [75, 76]. Another approach for dealing with different optical frequencies in non-linear effects employs antenna elements with different resonance wavelength matching the interacting optical fields [77]. The application of multifrequency gold nanowire antennas has been demonstrated in frequency conversion experiments.

2.4 Selected Applications of Surface Enhanced Vibrational Spectroscopy

2.4.1 SERS for Probing Catalytic Reactions

High molecular structural selectivity along with high detection sensitivity suggests surface enhanced vibrational spectroscopies as powerful methods for monitoring chemical processes and reactions.

Application of SERS for insight into catalytic processes requires bifunctional nanostructures that provide both plasmonic properties and the ability to act as catalyst. Direct observations of catalytic reactions have been reported by using composite nanoparticles with gold for plasmonic and Pt or Pd for catalytic function [78, 79].

In another experiment, gold nannoparticles and catalytic active Pt nanoparticles have been simultaneous immobilization on a glass surface, see schema a in Fig. 2.6 [80]. This approach combines the advantages of easy preparation without the need for synthesis of composite nanoparticles and high versatility regarding the choice of catalyst. The proximity of both types of nanoparticles enables interaction of the molecules with the platinum nanoparticles while they reside in the local optical fields provided by the localized surface plasmons of the gold nanoparticles. The

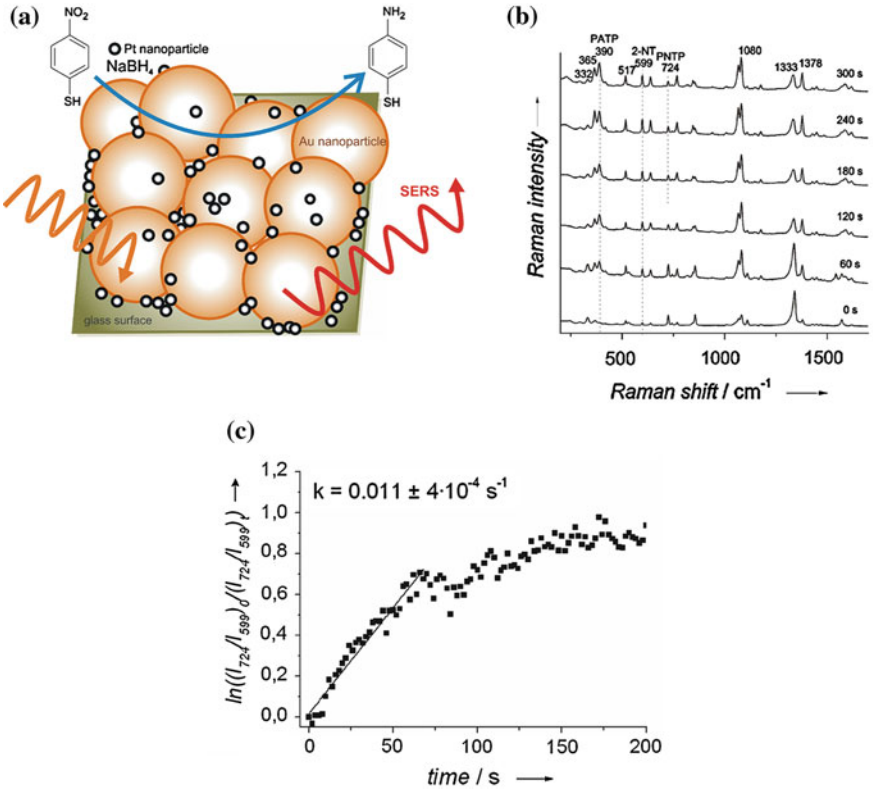

Fig. 2.6 SERS for probing the kinetics of nanoparticle-catalyzed reactions. **a** Schematic of a mix-and-match surface with immobilized gold and platinum nanoparticles. The reaction is catalyzed by the platinum nanoparticles, while the surface-enhanced Raman scattering (SERS) signal is brought about by local optical fields of the gold nanoparticles **b** SERS spectra for monitoring the reduction of *p*-nitrothiophenol (PNTP) by sodium borohydride to *p*-aminothiophenol (PATP), spectra were measured at different time points after the addition of sodium borohydride **c** Determination of rate constants for the reduction based on the intensity ratio of the band of PNTP at 724 cm^1 and of 2-NT at 599 cm^1 (Reprinted with permission from [80])

chemical species involved in the catalytic process can be characterized by their SERS features, see also Fig. 2.6b. To monitor the reaction over time, the relative intensity of typical SERS bands of the starting compound and the end product can be used for quantification, see Fig. 2.6c. Structural characterization of the species in the reaction and the rate constants are thus determined in the same experiment.

2.4.2 *Vibrational Spectroscopy of Protein Monolayers Using SEIRA*

Compared to SERS and particularly also compared to non-linear Raman methods, the electromagnetic contribution for SEIRA signals is "modest" since the effect is only proportional to the square of the field enhancement (see Fig. 2.3). However, IR absorption and Raman scattering follow different symmetry selection rules and can therefore probe different vibrational modes. For a comprehensive vibrational characterization, Raman scattering *and* IR absorption spectra are of interest.

As we have discussed, infrared absorption can be efficiently supported by nanoantenna arrays. The collective resonant excitation of the nanoantenna ensemble results in signal enhancement factors of $10^4 - 10^5$. This "collectively enhanced IR absorption" (CEIRA) spectroscopy technique allows direct identification of vibrational signatures of single protein monolayers of silk fibroin, see Fig. 2.7a. The ability to control the thickness of the silk protein films from several nanometers to several micrometers provides an opportunity to probe the near field behavior of the nanorod antenna by varying the film thickness. Due to the rapid decaying of the strongly enhanced near fields with distance from the nanorod surfaces saturation of the enhancement is expected to occur for films as thin as 40 nm. Figure 2.7b illustrates Amide-I and II vibrational modes of the protein back bone. These two vibrations also appear in the reflectance spectra shown in Fig. 2.7c. CEIRA is based on collective plasmonic excitations created by tailoring of the dipolar interactions in engineered nano-antenna arrays. The method allows detection of 300 zeptomoles of proteins for the entire array, corresponding to 145 molecules per antenna.

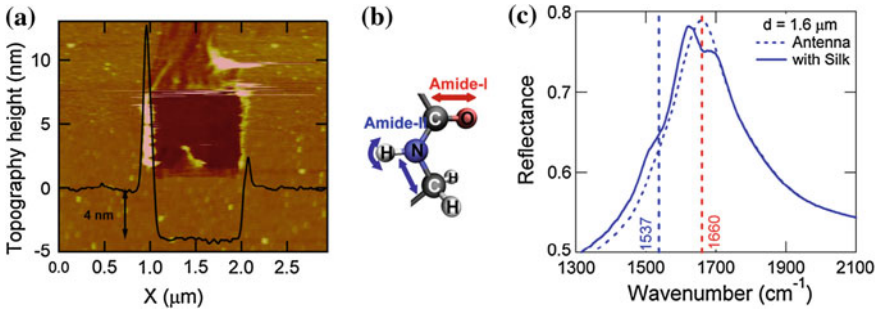

Fig. 2.7 Surface enhanced IR reflection absorption spectroscopy (IRRAS) of a single silk protein monolayer **a** Silk film thickness is measured by atomic force microscope for a 4 nm thick film. **b** Amide-I and II vibrational modes of the protein back bone. **c** Reflectance spectra from the nanoantenna array before (*dashed line*) and after coating of 2 nm thick protein film (*solid line*). *Dashed vertical lines* indicate the positions of the protein amide-I and II absorption peaks (Reprinted with permission from [7])

2.4.3 New Labels for Linear and Non-Linear Vibrational Probing and Imaging

During recent years, it has been demonstrated that surface-enhanced Raman scattering opens up exciting capabilities for creating new labels particularly for biosciences. Applications of SERS tags have been demonstrated for labeling DNA strands and proteins [81, 82], for in vivo imaging in a mice [83] and for probing and imaging in life cells [84, 85].

SERS labels consist of gold or silver nanoaggregates with an attached reporter species, e.g. a dye, see also Fig. 2.8. The labels are detected based on the SERS signature of the reporter molecule. Distinguishable spectral signatures even for similar reporter molecules enable a large pool of spectrally non-overlapping labels [3]. Since SERS works well with molecular non-resonant excitation, all labels can be used at the same excitation wavelength. Therefore, SERS labels benefit from real multiplexing capabilities.

As a particular advantage, SERS labels do not only highlight targeted structures through the specific reporter spectrum, SERS in the local optical fields of the gold or silver nanostructures also provides sensitive and spatially localized molecular

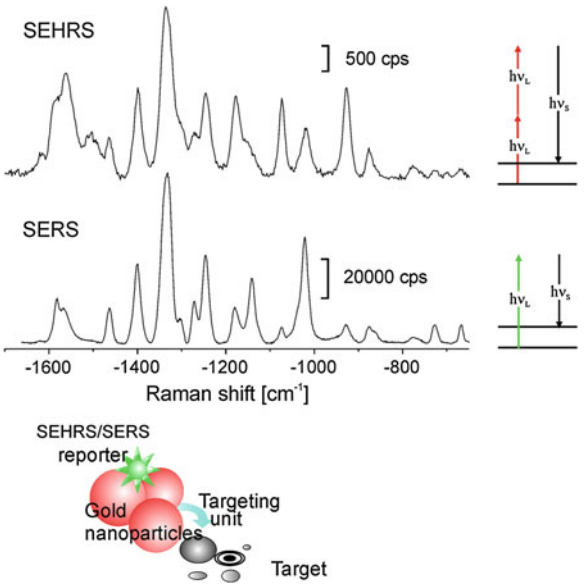

Fig. 2.8 Schematic of a multifunctional SERS label built from gold or silver nanoaggregates with an reporter molecule attached along with its one and two-photon excited spectral signature. The example shows SEHRS and SERS spectra from a label built from silver nanoaggregates with rose bengal as reporter molecule. Two-photon excited SEHRS spectra were measured using 1,064 nm mode locked ps pulses, one-photon excited SERS spectra were collected using 785 nm cw light (Reprinted with permission from [35])

structural information on the environment of the label [86]. Moreover, the SERS signature of a reporter molecule, attached to the gold nanoparticle, which exhibits a pH-sensitive Raman spectrum, can deliver information on the local pH-value in the surrounding of the label [87]. SERS labels can be functionalized (targeting unit) using specific linker in order to address specific molecules or structures.

Due to the plasmonic support, SERS appears at high signal level. This suggests SERS signatures for vibrational imaging.

Two-photon excitation is gaining rapidly in interest and significance in spectroscopy and optical imaging. The development of optical labels that are suitable also for two-photon excitation and non-linear imaging is an important task in advancing methods for vibrational probing and imaging. Effective plasmonic supported cross sections of SERS and SEHRS can be on the order of $10^{-17} - 10^{-16}\,\mathrm{cm}^2$ and $10^{-46} - 10^{-45}\,\mathrm{cm}^4\,\mathrm{s}$, respectively. This suggests versatile optical SERS/ SEHRS labels suitable for both one- and two-photon probing and imaging. Figure 2.8 shows the schematic of a SEHRS/SERS label along with its spectral signatures, for this label, SEHRS and SERS spectra of the reporter molecule rose bengal. Plasmonic supported Raman labels have also been employed in CARS imaging for immunohistochemistry [50].

2.5 Brief Summary and Outlook

Plasmonics supported vibrational spectroscopy can transform vibrational spectroscopy from a method for chemical structural analysis requiring relatively large amounts of matter to a tool for nanosciences providing at the same time high molecular structural selectivity and ultrasensitive detection limits. Vibrational spectra collected by surface enhanced Raman scattering (SERS), by surface enhanced infrared absorption (SEIRA), and by surface enhanced two-photon excited hyper Raman scattering (SEHRS) allow a comprehensive structural characterization of matter and monitoring of chemical processes. Sophisticated nanoantenna structures and arrays advance the field of surface enhanced IR absorption. Here, the extension to the THz range might be of particular interest. A combination of the confined probed volumes and the enhancement of vibratinal signatures in plasmonic fields with scanning probe capabilities of an atomic force microscope as it is employed in tip enhanced Raman spectroscopy enables simultaneous morphological-topological and molecular structural information at the nanoscale.

In particular, *non-linear* coherent and incoherent Raman scattering benefits from plasmonic support. Further progress in theoretical understanding of plasmonic enhancement as well as advanced technologies for making taylored plasmonic nanostructures will allow us to take advantage of all the potential capabilities of plasmonic supported non-linear vibrational spectroscopy. First observation of surface enhanced femtosecond stimulated Raman scattering opens up exciting new ways for probing ultrafast processes that might occur in plasmon-mediated interaction between molecules and light. Methods such as SEHRS, SEPARS and SECARS combine structural

sensitivity and selectivity of vibrational spectroscopy, methodological advantages of multiphoton and coherent spectroscopy, as well as high signal levels and confined probed volumes inherent to plasmon supported spectroscopy. Employing these advantages opens up exciting capabilities for vibrational probing and imaging.

References

1. B. Schrader, *Infrared and Raman Spectroscopy: Methods and Applications* (Wiley, Chichester, 1995)
2. D. Mitleman, *Sensing with Terahertz Radiation* (Springer, Berlin, 2003)
3. K. Kneipp, H. Kneipp, I. Itzkan, R.R. Dasari, M.S. Feld, Ultrasensitive chemical analysis by Raman spectroscopy. Chem. Rev. **99**, 2957–2975 (1999)
4. K. Kneipp, Surface-enhanced Raman scattering. Phys. Today **60**, 40–46 (2007)
5. P.L. Stiles, J.A. Dieringer, N.C. Shah, R.R. Van Duyne, Surface-enhanced Raman spectroscopy. Annu. Rev. Anal. Chem. **1**, 601–626 (2008)
6. J. Kneipp, H. Kneipp, K. Kneipp, SERS–a single-molecule and nanoscale tool for bioanalytics. Chem. Soc. Rev. **37**, 1052–1060 (2008)
7. R. Adato, A.A. Yanik, J.J. Amsden, D.L. Kaplan, F.G. Omenetto, M.K. Hong, S. Erramilli, H. Altug, Ultra-sensitive vibrational spectroscopy of protein monolayers with plasmonic nanoantenna arrays. Proc. Nat. Acad. Sci. U.S.A. **106**, 19227–19232 (2009)
8. V.N. Denisov, B.N. Mavrin, V.B. Podobedov, Hyper Raman scattering. Phys. Rep. **151**, 1 (1987)
9. A.M. Kelley, *Hyper-Raman scattering by molecular vibrations, in Annual Review of Physical Chemistry*, vol. 61 (Annual Reviews, Palo Alto, 2010), pp. 41–61
10. J.X. Cheng, X.S. Xie, Coherent anti-Stokes Raman scattering microscopy: instrumentation, theory, and applications. J. Phys. Chem. B **108**, 827–840 (2004)
11. C.W. Freudiger, W. Min, G.R. Holtom, B.W. Xu, M. Dantus, X.S. Xie, Highly specific label-free molecular imaging with spectrally tailored excitation-stimulated Raman scattering (STE-SRS) microscopy. Nat. Photonics **5**, 103–109 (2011)
12. C.L. Evans, X.S. Xie, Coherent anti-stokes Raman scattering microscopy: chemical imaging for biology and medicine. Annu. Rev. Anal. Chem. **1**, 883–909 (2008)
13. L. Dhar, J.A. Rogers, K.A. Nelson, Time-resolved vibrational spectroscopyin the impulsive limit. Chem. Rev. **94**, 157–193 (1994)
14. S. Umapathy, A. Lakshmanna, B. Mallick, Ultrafast Raman loss spectroscopy. J. Raman Spectrosc. **40**, 235–237 (2009)
15. A. Weigel, N.P. Ernsting, Excited Stilbene: intramolecular vibrational redistribution and solvation studied by femtosecond stimulated Raman spectroscopy. J. Phys. Chem. B **114**, 7879–7893 (2010)
16. R.R. Frontiera, R.A. Mathies, Femtosecond stimulated Raman spectroscopy. Laser Photonics Rev. **5**, 102–113 (2011)
17. M. Moskovits, *Surface-enhanced Raman spectroscopy: a brief perspective, in Surface-Enhanced Raman Scattering: Physics and Applications* (Springer-Verlag Berlin, Berlin, 2006), pp. 1–17
18. P. Johansson, H.X. Xu, M. Kall, Surface-enhanced Raman scattering and fluorescence near metal nanoparticles. Phys. Rev. B **72**, 035427 (2005)
19. M.I. Stockman, Nanoplasmonics: past, present, and glimpse into future. Opt. Express **19**, 22029–22106 (2011)
20. L. Novotny, N. van Hulst, Antennas for light. Nat. Photonics **5**, 83–90 (2011)
21. A. Ahmed, R. Gordon, Single molecule directivity enhanced Raman scattering using nanoantennas. Nano Lett. **12**, 2625–2630 (2012)
22. K. Kneipp, M. Moskovits, H. Kneipp, *in Surface-Enhanced Raman Scattering- Physics and Applications* (Springer, Berlin, 2006)

23. A. Otto, Surface- enhanced Raman scattering: 'classical' and 'chemical' origins, in *Light Scattering in Solids IV. Electronic Scattering, Spin Effects, SERS and Morphic Effects*, ed. by M. Cardona, G. Guntherodt (Springer, Berlin, 1984), pp. 289–418
24. A. Campion, P. Kambhampati, Surface-enhanced Raman scattering. Chem. Soc. Rev. **27**, 241–250 (1998)
25. J.R. Lombardi, R.L. Birke, Time-dependent picture of the charge-transfer contributions to surface enhanced Raman spectroscopy. J. Chem. Phys. **126**, 244709 (2007)
26. M.I. Stockman, *Electromagnetic theory of SERS, in Surface-Enhanced Raman Scattering: Physics and Applications* (Springer, Berlin, 2006), pp. 47–65
27. G.C. Schatz, M.A. Young, R.P. Van Duyne, *Electromagnetic mechanism of SERS, in Surface-Enhanced Raman Scattering: Physics and Applications* (Springer, Berlin, 2006), pp. 19–45
28. R.F. Aroca, D.J. Ross, C. Domingo, Surface-enhanced infrared spectroscopy. Appl. Spectrosc. **58**, 324A–338A (2004)
29. F. Neubrech, A. Pucci, T.W. Cornelius, S. Karim, A. Garcia-Etxarri, J. Aizpurua, Resonant plasmonic and vibrational coupling in a Tailored nanoantenna for infrared detection. Phys. Rev. Lett. **101**, 4 (2008)
30. A. Pucci, F. Neubrech, D. Weber, S. Hong, T. Toury, M.L. de la Chapelle, Surface enhanced infrared spectroscopy using gold nanoantennas. Phys. Status Solidi B Basic Solid State Phys. **247**, 2071–2074 (2010)
31. F. Le, D.W. Brandl, Y.A. Urzhumov, H. Wang, J. Kundu, N.J. Halas, J. Aizpurua, P. Nordlander, Metallic nanoparticle arrays: a common substrate for both surface-enhanced Raman scattering and surface-enhanced infrared absorption. ACS Nano **2**, 707–718 (2008)
32. V. Liberman, R. Adato, T.H. Jeys, B.G. Saar, S. Erramilli, H. Altug, Rational design and optimization of plasmonic nanoarrays for surface enhanced infrared spectroscopy. Opt. Express **20**, 11953–11966 (2012)
33. R. Hillenbrand, T. Taubner, F. Keilmann, Phonon-enhanced light-matter interaction at the nanometre scale. Nature **418**, 159–162 (2002)
34. M.S. Anderson, Enhanced infrared absorption with dielectric nanoparticles. Appl. Phys. Lett. **83**, 2964–2966 (2003)
35. J. Kneipp, H. Kneipp, K. Kneipp, Two-photon vibrational spectroscopy for biosciences based on surface-enhanced hyper-Raman scattering. Proc. Nat. Acad. Sci. U.S.A. **103**, 17149–17153 (2006)
36. H. Kneipp, K. Kneipp, F. Seifert, Surface-enhanced hyper-Raman scattering (SEHRS) and surface-enhanced Raman scattering (SERS) by means of mode-locked Ti:sapphire laser excitation. Chem. Phys. Lett. **212**, 374–378 (1993)
37. T. Itoh, Y. Ozaki, H. Yoshikawa, T. Ihama, H. Masuhara, Hyper-Rayleigh scattering and hyper-Raman scattering of dye-adsorbed silver nanoparticles induced by a focused continuous-wave near-infrared laser. Appl. Phys. Lett. **88**, 084102 (2006)
38. L. Weinan, A. Meyers-Kelley, SEHRS spectra on Ag films at pulse energies below 2 pJ. J. Am. Chem. Soc. **128**, 3492–3493 (2006)
39. K. Kneipp, Y. Wang, H. Kneipp, I. Itzkan, R.R. Dasari, M.S. Feld, Population pumping of ecited vibrational states by spontaneous surface-enhanced Raman scattering. Phys. Rev. Lett. **76**, 2444 (1996)
40. K. Kneipp, H. Kneipp, P. Corio, S.D.M. Brown, K. Shafer, J. Motz, L.T. Perelman, E.B. Hanlon, A. Marucci, G. Dresselhaus, M.S. Dresselhaus, Surface-enhanced and normal Stokes and anti-Stokes Raman spectroscopy of single-walled carbon nanotubes. Phys. Rev. Lett. **84**, 3470–3473 (2000)
41. K. Kneipp, H. Kneipp, R. Manoharan, I. Itzkan, R.R. Dasari, M.S. Feld, Surface-enhanced Raman scattering (SERS)—a new tool for single molecule detection and identification. Bioimaging **6**, 104–110 (1998)
42. K. Kneipp, H. Kneipp, I. Itzkan, R.R. Dasari, M.S. Feld, M.S. Dresselhaus, *Nonlinear Raman Probe of Single Molecules Attached to Colloidal Silver and Gold Clusters, in Optical Properties of Nanostructured Random Media* (Springer, Berlin, 2002)

43. W. Kiefer, D.A. Long, *Non-Linear Raman Spectroscopy and its Chemical Application* (Reider, Dordrecht, 1982)
44. A. Volkmer, J.X. Cheng, X.S. Xie, Vibrational imaging with high sensitivity via epidetected coherent anti-Stokes Raman scattering microscopy. Phys. Rev. Lett. **87**, 3901 (2001)
45. E. Liang, A. Weippert, J. Funk, A. Materny, W. Kiefer, Experimental observation of surface-enhanced coherent anti-Stokes Raman scattering. Chem. Phys. Lett. **227**, 115–120 (1994)
46. I. Baltog, M. Baibarac, S. Lefrant, Coherent anti-Stokes Raman scattering on single-walled carbon nanotubes and copper phthalocyanine thin films excited through surface plasmons. J. Opt. Pure Appl. Opt. **7**, 632–639 (2005)
47. I. Baltog, M. Baibarac, S. Lefrant, "Single-beam pumped" coherent anti-Stokes Raman scattering on carbon nanotubes thin films excited through surface plasmons. Physica E Low Dimensional Syst. Nanostruct. **40**, 2380–2385 (2008)
48. C.J. Addison, S.O. Konorov, A.G. Brolo, M.W. Blades, R.F.B. Turner, Tuning gold nanoparticle self-assembly for optimum coherent anti-stokes Raman scattering and second harmonic generation response. J. Phys. Chem. C **113**, 3586–3592 (2009)
49. C. Steuwe, C.F. Kaminski, J.J. Baumberg, S. Mahajan, Surface enhanced coherent anti-stokes Raman scattering on nanostructured gold surfaces. Nano Lett. **11**, 5339–5343 (2011)
50. S. Schlucker, M. Salehi, G. Bergner, M. Schutz, P. Strobel, A. Marx, I. Petersen, B. Dietzek, J. Popp, Immuno-surface-enhanced coherent anti-stokes Raman scattering microscopy: immunohistochemistry with target-specific metallic nanoprobes and nonlinear Raman microscopy. Anal. Chem. **83**, 7081–7085 (2011)
51. R.R. Frontiera, A.I. Henry, N.L. Gruenke, R.P. Van Duyne, Surface-enhanced femtosecond stimulated Raman spectroscopy. J. Phys. Chem. Lett. **2**, 1199–1203 (2011)
52. Y. Sonnefraud, A.L. Koh, D.W. McComb, S.A. Maier, Nanoplasmonics: engineering and observation of localized plasmon modes. Laser Photonics Rev. **6**, 277–295 (2012)
53. M.I. Stockman, Nanoplasmonics: the physics behind the applications. Phys. Today **64**, 39–44 (2011)
54. L. Novotny, From near-field optics to optical antennas. Phys. Today **64**, 47–52 (2011)
55. S. Lal, N.K. Grady, J. Kundu, C.S. Levin, J.B. Lassiter, N.J. Halas, Tailoring plasmonic substrates for surface enhanced spectroscopies. Chem. Soc. Rev. **37**, 898–911 (2008)
56. P.R. West, S. Ishii, G.V. Naik, N.K. Emani, V.M. Shalaev, A. Boltasseva, Searching for better plasmonic materials. Laser Photonics Rev. **4**, 795–808 (2010)
57. K. Kneipp, W. Yang, H. Kneipp, L.T. Perelman, I. Itzkan, R.R. Dasari, M.S. Feld, Single molecule detection using surface-enhanced Raman scattering (SERS). Phys. Rev. Lett. **78**, 1667–70 (1997)
58. K. Kneipp, H. Kneipp, J. Kneipp, Surface-enhanced Raman scattering in local optical fields of silver and gold nanoaggregatess–from single-molecule Raman spectroscopy to ultrasensitive probing in live cells. Acc. Chem. Res. **39**, 443–450 (2006)
59. K. Kneipp, H. Kneipp, R. Manoharan, E.B. Hanlon, I. Itzkan, R.R. Dasari, M.S. Feld, Extremely large enhancement factors in surface-enhanced Raman scattering for molecules on colloidal gold clusters. Appl. Spectrosc. **52**, 1493–1497 (1998)
60. K. Kneipp, H. Kneipp, V.B. Kartha, R. Manoharan, G. Deinum, I. Itzkan, R.R. Dasari, M.S. Feld, Detection and identification of a single DNA base molecule using surface–enhanced Raman scattering (SERS). Phys. Rev. E **57**, R6281–R6284 (1998)
61. M.I. Stockman, V.M. Shalaev, M. Moskovits, R. Botet, T.F. George, Enhanced Raman scattering by fractal clusters: scale-invariant theory. Phys. Rev. B **46**, 2821–2830 (1992)
62. V.A. Podolskiy, V.M. Shalaev, Giant optical responses in microcavity-fractal composites. Laser Phys. **11**, 26–30 (2001)
63. K.R. Li, M.I. Stockman, D.J. Bergman, Self-similar chain of metal nanospheres as an efficient nanolens. Phys. Rev. Lett. **91**, 227–402 (2003)
64. J. Kneipp, X.T. Li, M. Sherwood, U. Panne, H. Kneipp, M.I. Stockman, K. Kneipp, Gold nanolenses generated by laser ablation-efficient enhancing structure for surface enhanced Raman scattering analytics and sensing. Anal. Chem. **80**, 4247–4251 (2008)

65. C. Hoppener, L. Novotny, Exploiting the light-metal interaction for biomolecular sensing and imaging. Q. Rev. Biophys. **45**, 209–255 (2012)
66. N.J. Halas, S. Lal, W.S. Chang, S. Link, P. Nordlander, Plasmons in strongly coupled metallic nanostructures. Chem. Rev. **111**, 3913–3961 (2011)
67. J. Kundu, F. Le, P. Nordlander, N.J. Halas, Surface enhanced infrared absorption (SEIRA) spectroscopy on nanoshell aggregate substrates. Chem. Phys. Lett. **452**, 115–119 (2008)
68. V. Jayaraman, K.R. Rodgers, I. Mukeriji, T.G. Spiro, Hemoglobin allostery—resonance Raman spectroscopy of kinetic intermediates. Science **269**, 1843–1848 (1995)
69. K.R. Rodgers, T.G. Spiro, Nanosecond dynamics of the R–>T transition in hemoglobin-ultreviolet raman studies. Science **265**, 1697–1699 (1994)
70. E.J. Zeman, G.C. Schatz, An acurate electromagnetic theory study of surface enhancement factors for AG, AU, CU, LI, NA, AL, GA, IN, ZN and CD. J. Phy. Chem. **91**, 634–643 (1987)
71. G.H. Chan, J. Zhao, G.C. Schatz, R.P. Van Duyne, Localized surface plasmon resonance spectroscopy of triangular aluminum nanoparticles. J. Phys. Chem. C **112**, 13958–13963 (2008)
72. Z.L. Yang, Q.H. Li, B. Ren, Z.Q. Tian, Tunable SERS from aluminium nanohole arrays in the ultraviolet region. Chem. Commun. **47**, 3909–3911 (2011)
73. T. Dorfer, M. Schmitt, J. Popp, Deep-UV surface-enhanced Raman scattering. J. Raman Spectrosc. **38**, 1379–1382 (2007)
74. B. Ren, X.F. Lin, Z.L. Yang, G.K. Liu, R.F. Aroca, B.W. Mao, Z.Q. Tian, Surface-enhanced Raman scattering in the ultraviolet spectral region: UV-SERS on rhodium and ruthenium electrodes. J. Am. Chem. Soc. **125**, 9598–9599 (2003)
75. K. Kneipp, H. Kneipp, *Two-Photon Excited Surface-Enhanced Raman Scattering, Surface-Enhanced Raman Scattering: Physics and Applications* (Springer, Berlin, 2006)
76. K. Kneipp, H. Kneipp, SERS signals at the anti Stokes side of the excitation laser in extremely high local optical fields of silver and gold nanoclusters. Faraday Discuss. **132**, 27–33 (2006)
77. H. Harutyunyan, G. Volpe, R. Quidant, L. Novotny, Enhancing the nonlinear optical response using multifrequency gold-nanowire antennas. Phys. Rev. Lett. **108**, 4 (2012)
78. K.N. Heck, B.G. Janesko, G.E. Scuseria, N.J. Halas, M.S. Wong, Observing metal-catalyzed chemical reactions in situ using surface-enhanced Raman spectroscopy on Pd-Au nanoshells. J. Am. Chem. Soc. **130**, 16592–16600 (2008)
79. W. Xie, C. Herrmann, K. Kompe, M. Haase, S. Schlucker, Synthesis of bifunctional Au/Pt/Au Core/Shell nanoraspberries for in situ SERS monitoring of platinum-catalyzed reactions. J. Am. Chem. Soc. **133**, 19302–19305 (2011)
80. V. Joseph, C. Engelbrekt, J. Zhang, U. Gernert, J. Ulstrup, J. Kneipp, Characterizing the kinetics of nanoparticle-catalyzed reactions by surface-enhanced Raman scattering. Angew. Chem. Int. Ed. **51**, 7592–7596 (2012)
81. Y.W.C. Cao, R.C. Jin, C.A. Mirkin, Nanoparticles with Raman spectroscopic fingerprints for DNA and RNA detection. Science **297**, 1536–1540 (2002)
82. Y.C. Cao, R.C. Jin, J.M. Nam, C.S. Thaxton, C.A. Mirkin, Raman dye-labeled nanoparticle probes for proteins. J. Am. Chem. Soc. **125**, 14676–14677 (2003)
83. X.M. Qian, X.H. Peng, D.O. Ansari, Q. Yin-Goen, G.Z. Chen, D.M. Shin, L. Yang, A.N. Young, M.D. Wang, S.M. Nie, In vivo tumor targeting and spectroscopic detection with surface-enhanced Raman nanoparticle tags. Nat. Biotechnol. **26**, 83–90 (2008)
84. J. Kneipp, H. Kneipp, A. Rajadurai, R.W. Redmond, K. Kneipp, Optical probing and imaging of live cells using SERS labels. J. Raman Spectrosc. **40**, 1–5 (2009)
85. J. Kneipp, H. Kneipp, B. Wittig, K. Kneipp, Novel optical nanosensors for probing and imaging live cells. Nanomed. Nanotechnol. Bio. Med. **6**, 214–226 (2010)
86. J. Kneipp, *Nanosensors Based on SERS for Applications in Living Cells, Surface-Enhanced Raman Scattering: Physics and Applications* (Springer, Berlin, 2006)
87. J. Kneipp, H. Kneipp, B. Wittig, K. Kneipp, One and two photon excited optical pH probing for cells using surface enhanced Raman and hyper Raman nanosensors. Nano Lett. **103**, 17149–17153 (2007)

http://www.springer.com/978-94-007-7804-7

Plasmonics: Theory and Applications
Shahbazyan, T.V.; Stockman, M.I. (Eds.)
2013, XV, 577 p. 244 illus., 208 illus. in color.,
Hardcover
ISBN: 978-94-007-7804-7